ADVANCED FUNCTIONAL MATERIALS
www.afm-journal.de

Toward Robust Ionic Conductivity Determination of Sulfide-Based Solid Electrolytes for Solid-State Batteries

Fariza Kalyk, Lars Pescara, Marcel Drüschler, and Nella M. Vargas-Barbosa**

All-solid-state batteries (ASSBs) are taking the lead as the next-generation energy storage systems, mainly to the development of new solid electrolytes with high ionic conductivities (>1 mS·cm^{-1}) at room temperature. However, the robust quantification of the ionic transport of these materials is strongly influenced by sample processing, contacting and cell setups. The aim of this study is to evaluate the robustness of the extracted ionic conductivity of sulfide-based solid electrolytes using lithium argyrodite (Li_6PS_5Br) as a model system, with particular attention to the influence of sample processing parameters and measurement conditions. The impact of isostatic and uniaxial processing pressures, contact material, measurement and analyses conditions of electrochemical impedance spectroscopy (EIS) is systematically evaluated employing three different measurement cell setups. The findings underscore the necessity for standardized protocols in characterizing solid electrolytes. By establishing a comprehensive methodology for the evaluation of ionic conductivities, this work aims to facilitate the reliable application of solid electrolytes in ASSBs.

1. Introduction

The rapid development in battery technologies, especially in the context of renewable energy storage and electric vehicles, drives the need for more efficient, longer lasting, and safer batteries. Lithium-ion batteries have dominated the market, but new technologies, particularly solid-state batteries, are emerging as promising alternatives.[1–3] All-solid-state batteries (ASSBs) are considered one of the most promising next-generation energy storage devices. They offer potential advantages over conventional lithium-ion batteries, such as higher energy density, when incorporating Li metal or Si as a negative electrode, and the possibility of bipolar stacking due to the solid electrolyte separator.[3,4] However, there are a number of challenges to fully implement ASSBs, one of which is the lack of standardized protocols to determine the performance of the battery components, both at the material- and cell-level. We recently reported on an international interlaboratory study on the comparability and reproducibility of ASSBs cell cycling performance.[5] The large differences observed in cell cycling performance were partially explained by the significant variability of cell assembly protocols among the participating groups, which emphasizes the importance of comprehensive reporting and demonstrating the reproducibility of the results by reporting triplicate data. Another obstacle to the implementation of ASSBs is the limited commercial and large-scale availability of solid electrolytes (SEs). Although the investigation and optimization of SEs with high ionic conductivity (>10^{-2} S·cm^{-1} at room temperature), and good electrochemical stability against electrode materials have been a major focus of research,[6–10] the absence of standardized methodology for the benchmarking on SEs hinders the comparability. In general, measuring the ionic conductivity of a SE is not complicated: a sample with fixed dimensions is contacted with two electrodes, also of fixed dimensions, against which the SE sample is stable, and a frequency-dependent impedance measurement at open circuit voltage is performed to determine the total resistance of the sample (**Figure 1a**). Then, considering the dimensions of the sample (thickness and electrode area), a cell constant is determined to convert the value of the resistance to an ionic conductivity (σ_{ion}, Equation 1):

$$\sigma_{ion} = \frac{d}{R \cdot A} \tag{1}$$

where σ_{ion} is the ionic conductivity (S·cm^{-1}), d is the thickness of the sample (cm), R is the total resistance (Ω), and A is the electrode area (cm^2).

However, various different factors can influence the reported ionic conductivity values. A recent interlaboratory Round

F. Kalyk
Institute of Energy Materials and Devices (IMD)
IMD-4: Helmholtz-Institute Münster
Forschungszentrum Jülich
48149 Münster, Germany
E-mail: f.kalyk@fz-juelich.de

L. Pescara, M. Drüschler
rhd instruments GmbH & Co. KG
Otto-Hesse-Strasse 19 T3, 64293 Darmstadt, Germany

N. M. Vargas-Barbosa
Chair of Electrochemistry and Bavarian Center for Battery Technology (BayBatt)
University of Bayreuth
Universitätstrasse 30, 95448 Bayreuth, Germany
E-mail: n.vargas-barbosa@uni-bayreuth.de

The ORCID identification number(s) for the author(s) of this article can be found under https://doi.org/10.1002/adfm.202509479

DOI: 10.1002/adfm.202509479

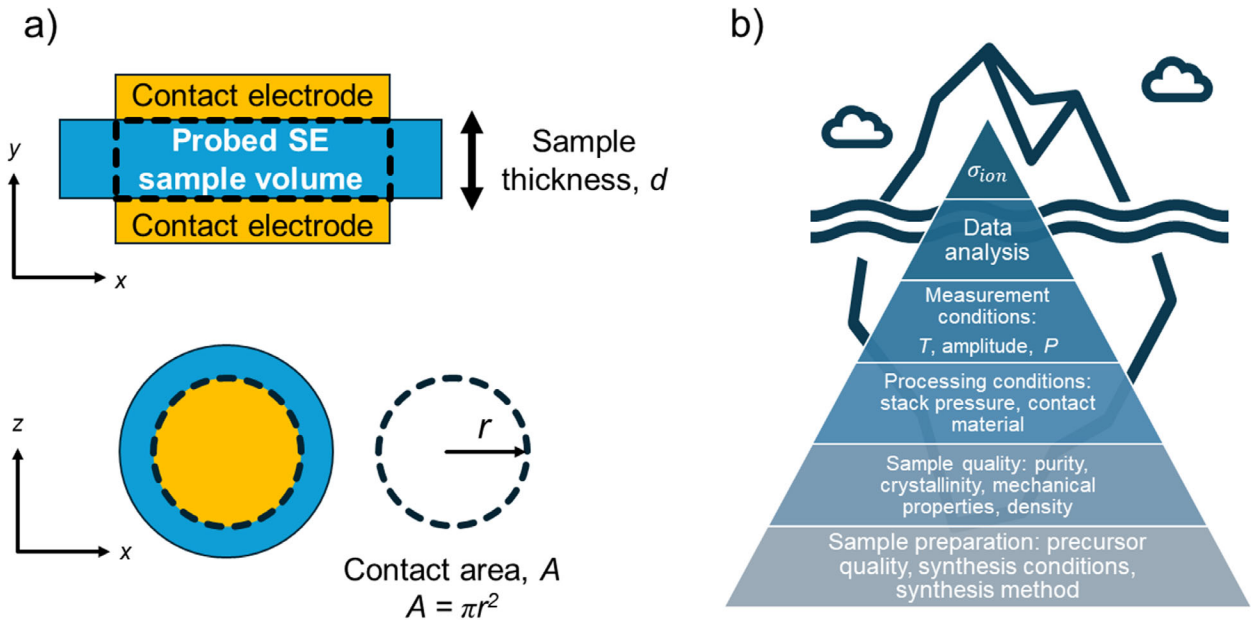

Figure 1. a) Schematic representation of the sample configuration; b) the schematics of the factors influencing the total ionic conductivity values.

Robin study[11] reported the reproducibility of ionic conductivity measurements in superionic lithium thiophosphate solid electrolytes. Although all groups received nominally equal samples, a range of up to ± 50% from the calculated average ionic conductivity was established. In the latter study, it was difficult to ascertain which parameter contributed the most to the observed variation. Nonetheless, sample processing was proposed to play the largest role in this type of materials.[11] This hypothesis was recently verified by Perrenot et al.[12] where they evaluated the effect of the uniaxial compression pressure and compression time on the resulting ionic conductivity of Li_3PS_4. Although the expected trend of higher ionic conductivities correlating with higher compression pressures was observed, this study shows that the resulting microstructure of the SE samples, i.e., the distribution and average size of the pores which were influenced by the compression time, strongly influence the attained ionic conductivities. To complicate matters further, Cronau and coworkers[13] showed that the applied pressure during the measurement, and not just during sample processing, can strongly influence obtained sample resistances in microcrystalline sulfide-based SEs. Taken together, these studies show that the standardization of ionic transport measurements is necessary to enable comparability of current and new SEs as they are developed and optimized for applications in ASSBs. Such standardized protocols will aid not only lab-scale research, but also quality control of upscaled solid electrolyte materials that are implemented in ASSB production lines.

A recent report by Krasnikova and coworkers[14] outlines a protocol for standardizing the determination of ionic conductivity measurements in solid electrolyte samples. However, its applicability is mostly limited to oxide-based ceramic ionic conductors ($Li_{1.3}Al_{0.3}Ti_{1.7}(PO_4)_3$ is their model sample) and does not systematically evaluate the effect of applied pressure prior and during the measurement on the resulting sample resistance. Similarly, a study by Müller and coworkers[15] proposes a harmonized sample testing and data analysis procedure that results in differences of <2% and <3% for the ionic conductivities of $Li_{6.45}La_3Zr_{1.6}Ta_{0.4}Al_{0.05}O_{12}$ and $Li_{1.3}Al_{0.3}Ti_{1.7}(PO_4)_3$ samples, respectively, if all samples and cells are prepared by the same group and the exact same measurement procedure is used.

Although the impedance measurement conditions can influence the quality and resulting data from which the ionic conductivity is extracted, we are not aware of a systematic considering it along with sample processing. The perturbation amplitude is a critical parameter that can influence the accuracy and reliability of the measurement results.[16,17] If the perturbation amplitude is too high, it can induce non-linear behavior between the applied signal and the response of the electrochemical system, leading to distorted impedance data.[18] A too-low perturbation amplitude might not be sufficient to generate a measurable response, leading to a poor signal-to-noise ratio.[17] Moreover, to standardize the analyses of the data and improve the reproducibility, it is important to report not only the obtained data but the way it was measured and analyzed. Since the conductivity is dependent on the data extracted from the equivalent circuit used for the fitting of the spectra, the choice of the equivalent circuit and the quality of the fit play a large role and should be comprehensively reported.[18–22]

As material scientists, we tend to focus on the influence of synthesis conditions of our target material on a specific figure of merit, which in the case of solid electrolyte is the ionic conductivity. However, our figure of merit is essentially the tip of an iceberg (Figure 1b): the material (usually powdered) needs to be processed so that electrode contacts can be applied, then the processed sample needs to undergo impedance measurements, and the acquired data needs to be analyzed. Each of the latter steps influence the final value we obtain for the ionic conductivity of our sample and to our knowledge, there is no single report that addresses all steps comprehensively in a single sample. To address this knowledge gap, we designed and conducted a systematic study to evaluate the effect of *sample processing*,

the *measurement parameters*, and *data analysis protocol* on the resulting ionic conductivity of SE samples.

Recent studies have highlighted the critical role of processing pressure in optimizing the performance of sulfide-based solid electrolytes. Wang et *al.*[23] demonstrated that hot-pressing Li_6PS_5Cl at 200 °C applying 450 MPa helps to achieve near-theoretical densification, resulting in high ionic conductivity that remains stable even under low external pressures during operation. Complementing this, Faka et *al.*[24] investigated the effect of internal strain on ionic conductivity of Li_6PS_5Br by applying various extremely high pressures, up to 10 GPa. Their findings reveal that activation volumes for Li^+ migration increase with higher degrees of Br^-/S^{2-} site disorder and indicates that structural disorder influences the pressure sensitivity of ionic transport. Moreover, this study demonstrates the potential of strain engineering as an effective method for tuning the ion conductivity without altering the composition of the material. Additionally, Tran et *al.*[25] optimized the synthesis and processing conditions of Li_6PS_5Cl separator tapes for ASSBs focusing on the effect of particle size distribution and applied uniaxial densification pressure (up to 1 GPa). A threshold pressure of ≈350 MPa was identified where the ionic conductivity significantly increases and a maximum densification was achieved. Sakuda et al.[26] reported that pressures above 300 MPa improved the density and conductivity of $75Li_2S{\cdot}25P_2S_5$ type electrolyte. Sedlmeier et al.[27] investigated the influence of time and pressure on Li_6PS_5Cl, $Li_7P_3S_{11}$, and $Li_{10}SnP_2S_{12}$ separator sheets and reported decrease of porosity from 50% to 3–12% (depending on the separator) and increase in conductivity at pressures of 590 MPa. Ates et al.[28] fixed 300 MPa to compress four bathes of β-Li_3PS_4 with different particle size, shape and porosity. Authors reported that the sample with the highest porosity and largest particle size had highest conductivity and most stable cycling performance. Kim et al.[29] achieved room temperature conductivity of 4 $mS{\cdot}cm^{-1}$ for $Na_{11}Sn_2PS_{12}$ which was isostatically pressed at 370 MPa for 3 min using a battery press cell. Huang et al.[30] mixed very expensive $Na_2B_{10}H_{10}$ with more affordable $Na_2B_{12}H_{12}$ in a 1:1 and 1:3 ratio and pelletized using a hydraulic press at pressure between 65 and 2080 MPa. Authors have concluded that by applying suitable pressure the cost for the desired SE can be reduced to 25% (500 MPa for ratio of 1:1 and 1 GPa for ratio 1:3).[30] PEO-based polymer electrolytes show a twice increase in ionic conductivity, decrease of activation barriers alongside improved battery cell performance after cold-rolled in a roller press under the line loading of 150 $N{\cdot}mm^{-1}$ (≈150 MPa).[31] Mormeneo-Segarra et al.[32] achieved high ionic conductivity and low activation energies for $Li_{1.3}Al_{0.3}Ti_{1.7}(PO_4)_3$ electrolyte after cold-sintered at 400 MPa and 200 °C with $LiOH/LiNO_3$ hydroflux. Collectively, these findings highlight that mechanical densification through high-pressure processing, typically between 100 MPa and 1 GPa, plays a role in the electrochemical performance of solid electrolytes.

As a model system we used the thiophosphate-based Li_6PS_5Br SE due to its relatively high ionic conductivity at room temperature (ca. 10^{-3} $S{\cdot}cm^{-1}$), stability, tunable properties, cost-effectiveness, and reduced interfacial resistance against lithium metal.[33–36] Via thorough evaluation of *processing conditions*, *measurement pressure*, *contact material*, and *the measurement conditions* we have generated an unprecedently large dataset of impedance spectra for Li_6PS_5Br. The spectra were comprehensively and systematically analyzed using equivalent circuit models to help us suggest a standardized protocol for the characterization of similar powdered SE samples. Therefore, this work established a foundation for standardizing ionic transport quantification in solid electrolytes, and offers high-quality spectra that can be reused further to develop software for faster, more accurate analysis and automated spectra fitting.

2. Experimental Section

All processing and sample treatments of Li_6PS_5Br (LPSBr) were carried out under argon atmosphere. Lithium sulfide (Li_2S, Thermo Scientific Chemicals, 99.9%), phosphorus pentasulfide (P_2S_5, Sigma–Aldrich, 99%), and LiBr (Sigma-Aldrich, 99.995%) were mixed according to the necessary stoichiometric ratio for the target material in an amount of 2 g per synthesis batch. The precursor mixture was hand-ground in an agate mortar, pressed into pellets and placed in carbon-coated quartz ampoules (10- or 12-mm inner diameter and 10–12 cm in length), which were sealed under vacuum and allowed to react at 550 °C for 2 weeks. The carbon coating (done by carbonizing acetone at high temperatures) minimizes trace water and oxygen in the reaction atmosphere and serves as the protective buffer between the argyrodite and the quartz. After additional cleaning of the carbon-coated ampules they were pre-heated at 800 °C for 2 h under dynamic vacuum. After synthesis, the material was subsequently ground and characterized using X-Ray Diffraction (STOE STADI P diffractometer, λ (Cu $K_{\alpha 1}$,) Mythen4K detector in Debye–Scherrer scan mode at room temperature) and Raman spectroscopy (Bruker Senterra, equipped with a 532 nm excitation laser). Raman spectra in the range of 47–1548 cm^{-1} were measured with a laser power of 2.5 mW, an integration time of 1000 s and four co-additions. The obtained data was processed with the OPUS 7.5 software. After confirming purity of the samples, powders were isostatically pressed at the following pressures: 160 MPa (P_1), 235 MPa (P_2), and 320 MPa (P_3), for 40 min, at room temperature (25 °C), using a 12 mm diameter pressing tool. To evaluate the influence of the electrode contact material, sputtered gold, sputtered platinum and indium foil were used. The choice of electrodes considered was motivated by the workplan in the proposal that funded this project. Moreover, gold and platinum are commonly used as contact materials, whereas indium has the advantage that it can be purchased and is soft enough to enable good contact with the sample with minimal applied pressure. The diameter of electrodes was set to 8 mm (**Figure 2a**). The pellet thickness was measured using a calliper with an accuracy of 0.02 mm. Since calculating conductivity requires the dimensions of the probed sample volume and resistance values obtained from fitting, the error on the ionic conductivity of a single pellet can arise from the uncertainties in thickness, electrode diameter, the errors in the fitted resistance values and the error in the temperature at which the measurement was done. An example of the error propagation for the calculation of the ionic conductivity is detailed in the Supporting Information. Moreover, the comparison of the error of a single pellet is compared to the average of three nominally equal pellets (Figure S3, Supporting Information). Based on these data, we can confidently state that the largest contributor to the error on the calculation of the ionic conductivity of a single pellet is the uncertainty in the sample's thickness.

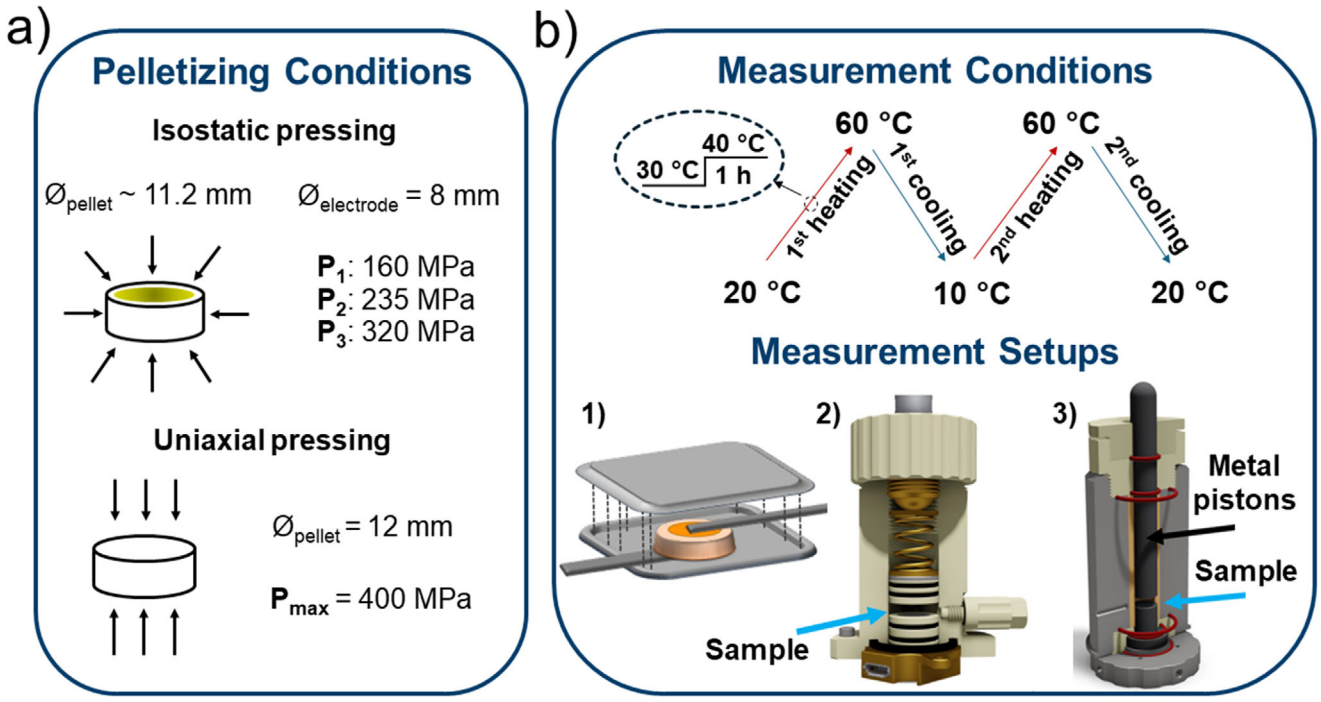

Figure 2. Schematic representation of Li_6PS_5Br electrolyte a) sample processing conditions, b) electrochemical impedance spectroscopy measurement conditions and setups, where 1) pouched cell, 2) TSC-battery cell, and 3) CompreCell 12C.

Electrochemical impedance spectroscopy (EIS) was used to measure ionic conductivities of solid electrolytes in the temperature range from 10 to 60 °C with 1 h equilibration time at each step using a VMP300 impedance analyser (Biologic Science Instruments) at frequencies from 1 MHz to 100 mHz with various sinusoidal excitation amplitudes of 10, 50, and 100 mV (peak-to-peak voltage). A NEISYS analyser (Novocontrol Technologies GmbH & Co. KG) was coupled with CompreCell 12 C at frequencies from 1 MHz to 0.1 Hz and amplitudes of 10, 50, and 100 mV root mean square (RMS). A schematic of the electrochemical protocol used for all samples is shown in Figure 2b and Figure S1 (Supporting Information).

All samples were prepared in triplicate at each processing pressure to evaluate the reproducibility of the data and the impedance measurements were performed with two heating and cooling cycles per measurement (Figure 2b). Moreover, three setups were used to study the influence of the pressure applied during the measurement. The first measurement setup is a pouched cell with minimal applied pressure during the measurement. Pressed pellet with sputtered Au electrodes is placed between two aluminum current collectors and enclosed in a pouch under Ar. Clamps are applied on the pouched cell to ensure a better contact (Figure 2b; Figure S1, Supporting Information). The second measurement setup is the TSC-battery cell (rhd instruments GmbH & Co. KG) which contains a spring with a constant 128 N contact force. This ensures that some pressure is maintained during measurements on the pre-pressed and contacted electrolyte, which is placed between two electrodes made of stainless-steel press-fitted in PEEK (Figure 2b). The third measurement setup (Figure 2b) is a computer-controlled uniaxial press (CompreDrive, rhd instruments GmbH & Co. KG) with electrochemical test cell CompreCell 12C (rhd instruments GmbH & Co. KG) that allows simultaneous temperature and pressure control. For each experiment, a small amount of powder (ca. 70–120 mg) was placed in the 12 mm diameter mold, sealed under Ar, and measured in the CompreDrive setup. Temperature was regulated via a fluid jacket connected to an external circulator (HUBER Unistat 405, Peter Huber Kältemaschinenbau SE). Powder was gradually densified from 10 to 400 MPa at a constant 25 °C, with impedance spectra taken 90 s after each stable pressure step. The process was repeated on the densified sample to determine the optimal pressure for good electrical contact. This optimal pressure (usually in the range of 200 MPa for the samples studied here) was then used for temperature-dependent measurements from −10 °C to 60 °C, with 30 min equilibration at each step.

All impedance spectra were fitted applying the appropriate electrical equivalent circuits (examples of the circuit are depicted in Figure S3, Supporting Information) using the RelaxIS 3 software (rhd instruments GmbH & Co. KG). RelaxIS 3 software supports various weighting modes, which influence the fit of the data in different ways. Weighting mode adjusts the dataset range that most strongly influences the fit by assigning a factor to the real and imaginary parts of the measured impedance.[37] In our case, the chosen mode weighs the data points by log_{10}^2 favoring high frequency range.[37] Different frequency ranges were used for the fitting of the same sample to see the influence of the selected frequency range on the resulting total ionic conductivities. Proportional weighing mode was used for the evaluation of data obtained from 3rd measurement setup.

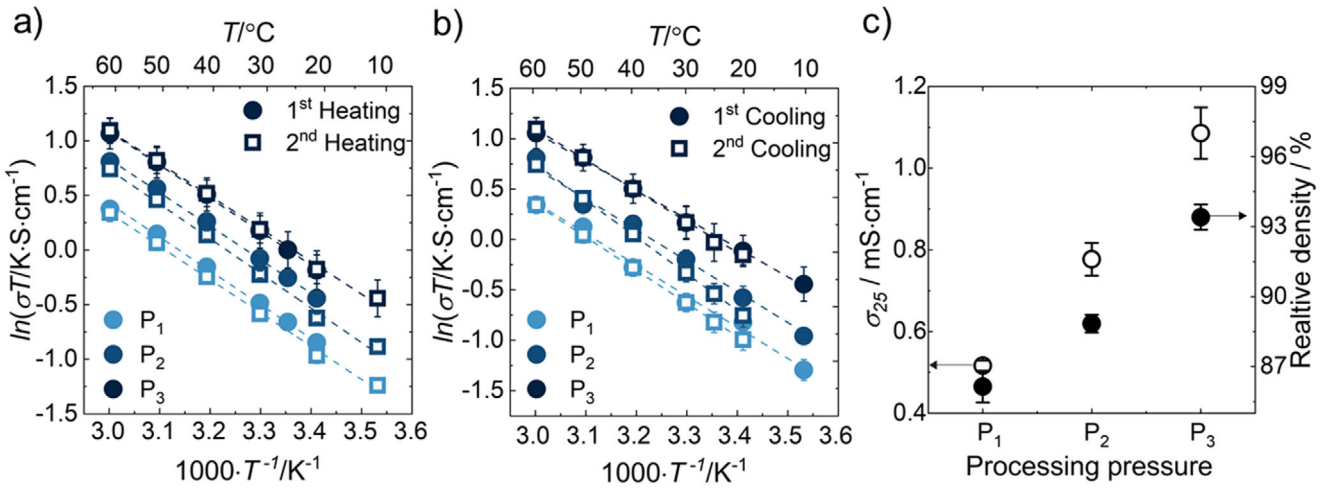

Figure 3. Arrhenius plots of total ionic conductivities of the average of multiplicate measurements under nominally equal conditions at a) 1st/2nd heating and b) 1st/2nd cooling cycles measured in a pouched cell. Dashed lines are the linear fits to the data. c) Average total ionic conductivities of multiplicate measurements at 25 °C and average relative densities as a function of the processing pressure. Each data point represents the average value of the total ionic conductivity of three pellets per processing pressure and the error bars correspond to the standard deviation of those three pellets. The processing pressures are 160 MPa (P_1), 235 MPa (P_2), and 320 MPa (P_3).

3. Results and Discussion

3.1. Effect of Processing Pressure

Li_6PS_5Br pellets were isostatically pressed at 160, 235, and 320 MPa (P_1, P_2, and P_3, respectively). The deconvolution of bulk and grain boundary contributions is not possible in this type of electrolytes in the measured temperature range and therefore, the conductivities shown here correspond to the total ionic conductivity of the samples. The impedance spectra of all pellets can be found in (Figures S7–S15, Supporting Information). **Figure 3**a,b show the Arrhenius plots of average total ionic conductivities of multiplicate measurements under nominally equal conditions measured in a pouched cell. As the pelletizing pressure increases, the relative density of the pellets also increases 86 ± 0.7% at P_1, 89 ± 0.4% at P_2, and 93 ± 0.5% at P_3, and a similar trend is observed for the total ionic conductivity of Li_6PS_5Br samples (Figure 3c). Namely, pellets pressed at P_3 exhibited the highest ionic conductivity and lowest activation energy (E_a) across all cycles and temperatures (Table S2, Supporting Information), with σ_{total} = 1.09 ± 0.06 mS·cm^{-1} at 25 °C and E_a = 0.258 ± 0.003 eV, compared to 0.52 ± 0.01 mS·cm^{-1} and 0.271 ± 0.002 eV for P_1. The obtained results align well with previously reported values in the literature. Kraft et al.[36] report values in the order of 1 mS·cm^{-1} on LPSBr samples processed via uniaxial compression at 3 tons (≈380 MPa) for 3 min, demonstrating the comparability of uniaxial and isostatic sample processing conditions. Yu et al.[40] pelletized LPSBr at ≈294 MPa and reported a high conductivity of 2.58 mS·cm^{-1} which was achieved due to subsequent sintering of the pellet at 500 °C for 24 h. Zhou et al.[41] achieved a room temperature conductivity of 1.9 mS·cm^{-1} for the solution-engineered Li_6PS_5Br. Gautam et al.[42] reported room temperature conductivities between 0.5 and 2 mS·cm^{-1} depending on the site-disorder of the slow-cooled Li_6PS_5Br samples. Applying "high enough" pressures during sample processing can help increase density and mechanical strength, ensure material homogeneity, and potentially increasing the conductivity.[38,39] Our results further emphasizes the critical role of the processing pressure and the need for its optimization in the characterization of solid electrolytes. From our results we suggest using isostatic processing at 320 MPa on sulfide-based SEs.

3.2. Effect of Electrode Material

The electrode material used for contacting the sample in EIS measurements plays an important role due to potential variations in interfacial resistance and contact stability.[15] In this study, we tested three different types of electrodes: sputtered gold (Au), sputtered platinum (Pt), and an indium (In) foil on samples prepared at P_3 (**Figure 4**). As expected, the type of electrode significantly influenced the measured impedance response (Figure 4b), sputtered Au and Pt, being noble and relatively inert, acted as blocking electrodes with minimal reactivity with the electrolyte material. Both sputtered electrodes provided consistent and reproducible results, moreover the extracted conductivity values were in close agreement, indicating that either material is suitable for reliable conductivity measurements. In contrast, measurements using In foil resulted in significantly lower total ionic conductivities, nearly half of those measured with sputtered contacts. This discrepancy is attributed not only to the electrochemically active nature of In, which can form alloys with Li, but more critically to the mechanical and geometrical limitations of using foil as an electrode. Indium is a soft metal, and when pressed against the electrolyte, it tends to deform or smear across the surface, making it difficult to define a clear and consistent contact area. This results in poor contact and introduces variability in interfacial resistance which affects the reproducibility. Our findings underscore not only the importance of the choice of electrode material but also the method of contacting it to the electrolyte for accurate and reproducible conductivity determination. Sputtering offers a clear advantage by providing uniform coverage, ensuring

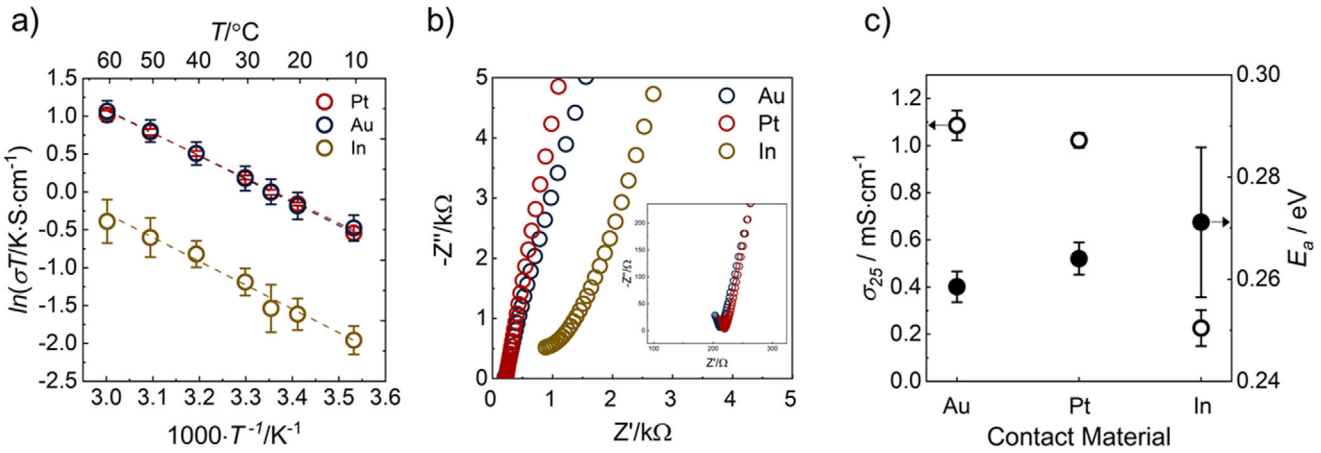

Figure 4. a) Arrhenius plots of total ionic conductivities of Li_6PS_5Br sample pelletized at 320 MPa and measured at 10 mV perturbation amplitude in a pouched cell, first cooling cycle. Dashed lines are the linear fits to the data. b) Nyquist plots of Li_6PS_5Br samples measured at 25 °C pelletized at 320 MPa with different electrode materials. c) Comparison of the ionic conductivities of the average of triplicate measurements at 25 °C and activation barriers as a function of contact material. The error bars represent the standard deviation of three pellets per processing pressures.

better-defined electrode – electrolyte interfaces and minimizing contact issues.

3.3. Effect of Frequency Range on Fit Quality and Resulting Resistivity

Impedance spectra are often analyzed by considering equivalent electrical circuit models made up of physical circuit elements such as resistors, capacitors, inductances and constant phase elements (CPEs). Here, such circuit elements are meant to describe electrochemical processes, e.g. a pure resistor can describe the movement of ions due to the applied electric field, whereas a capacitor can represent the dielectric properties of the sample. For solid ionic conductors, a parallel combination of resistors and CPEs (to account for non-idealities in the dielectric and capacitive properties of the samples) are usually considered. In the case of good solid electrolytes, such as the argyrodites studied here, it is sometimes difficult to choose the "correct" equivalent circuit model because the total impedance of the cell is often dominated by the low-frequency electrode polarization process (which is mostly unrelated to the ion transport taking place in the bulk of the material). Within this study, we restricted our data analysis primarily to only two possible equivalent circuits model (insets in Figure S4, Supporting Information). We have chosen the equivalent circuit that consists of the resistor in parallel with a CPE to model the single arc observed at high frequencies, and a separate CPE to describe the data in the low-frequency range (beyond the arc). The arc corresponds to both the bulk and grain boundary response of the solid electrolyte, where the resistor models the total ionic resistance and the CPE accounts for the fact that both processes are contributing to that arc. The distinction of bulk and grain boundary contributions in argyrodite-type solid electrolyte samples is typically only possible at temperatures below −60 °C.[11] The low-frequency tail represents the blocking electrodes, which are well-described by the additional CPE element (Figure S4, Supporting Information). Note that at higher temperatures, the resolution of the high-frequency arc is no longer possible due to a limited number of data points. Therefore, for these spectra a resistor connected in series with a CPE was considered to capture the total resistivity of the sample and the electrode blocking behavior at low-frequencies as before.

Figure 5 shows spectra fitted weighing the data points using a log_{10}^2 function at different frequency ranges. The quality of the fit, represented by chi-square (X^2), changes depending on the frequency limits chosen for the fit. When fitting the results with the full frequency range used for the measurement (1 MHz–0.1 Hz, Figure 5a) the X^2 has a significantly larger value. Both Figure 5b,c, show X^2 values below 10, indicating a good match between the experimental and fitted data. This is more clearly reflected if we consider how the absolute error of the resistance values of the fit vary as the frequency range is adjusted: for the full spectrum we obtained 256 ± 11 Ω (Figure 5a), whereas 280.7 ± 0.3 Ω and 279.1 ± 0.2 Ω are obtained for the spectra in Figure 5b,c, respectively. A difference of tens of Ω might not seem like a lot, but since these materials are meant to be implemented as thin separators (ca. 20 µm thick), prepared from large batches, such a difference can influence decisions about implementation and sample quality control upon upscaling. Note that, although better X^2 values are obtained when discarding low frequency datapoints, the influence of any electrode processes is neglected. The latter might not be desired when it is unclear if the solid electrolyte sample is stable against the electrode materials used and/or when there is interest in evaluating any interfacial processes for a particular sample.

3.4. Effect of Perturbation Amplitude

The correct perturbation amplitude helps in obtaining consistent and comparable impedance measurements. At low frequencies, higher amplitudes might be necessary to avoid noise, while at high frequencies, lower amplitudes might be sufficient to generate a reasonable response and prevent nonlinear effects.[16] Since the applied amplitude can cause non-linear behavior, the linearity of the system was checked using two methods. First, a practical

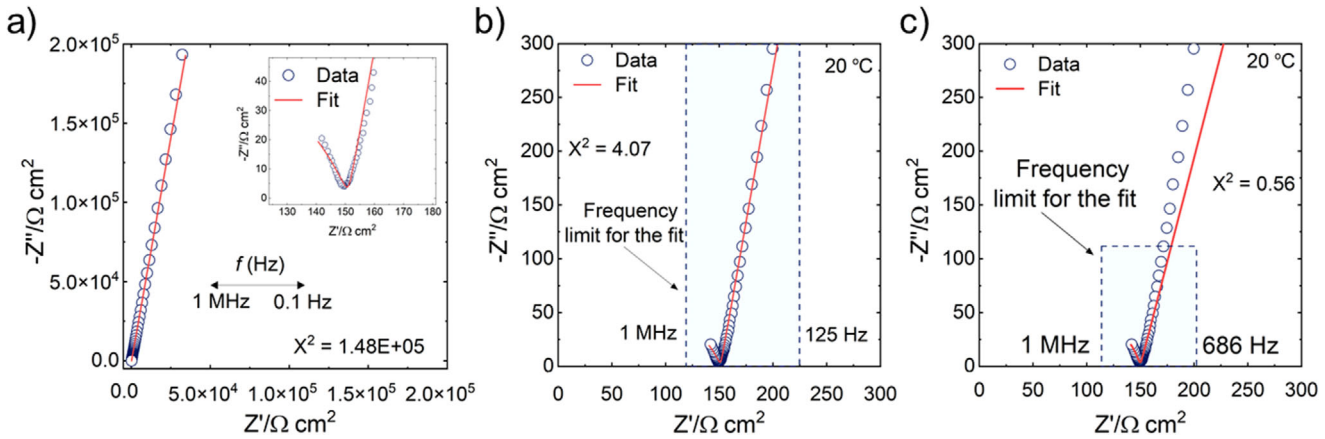

Figure 5. Representative Nyquist plots for a Li_6PS_5Br sample pelletized at 320 MPa and measured at 20 °C using a 10 mV amplitude in a pouched cell for fitting the electrical equivalent circuit model in Figure S4 (Supporting Information) considering various frequency ranges a) full frequency range measured, i.e., 1 MHz to 0.1 Hz, b) adjusted lower frequency limit up to 125 Hz, and c) adjusted lower frequency limit up to 686 Hz.

test of the linearity, where the measurement of the same sample ran within the selected frequency range and repeated with the reverse range, was performed (Figure S5, Supporting Information). Considering that the impedance of the linear system should be independent of the amplitude, the EIS data are expected to be identical.[18] The obtained results show that the spectra of pellets measured at 10 and 100 mV were identical at all frequencies. Whereas the spectra of pellets at 50 mV had different tail at the lower frequencies indicating the possible non-liner behavior (Figure S5, Supporting Information). Second, total harmonic distortion (THD) was employed to evaluate the linearity of the impedance data (Figure S6, Supporting Information). As reported previously and generally considered, a THD parameter larger than 4% can be considered as non-linear system.[17–20,43] All measurement amplitudes result in THD values below 1% (Figure S6, Supporting Information), indicating the linearity of the system.

Figure 6a presents the results obtained from the Li_6PS_5Br samples pelletized at the P_3 and measured at 10, 50, and 100 mV perturbation amplitudes. At higher temperatures and higher frequencies, the differences between amplitudes are negligible, whereas more dispersion is evident at lower temperatures and lower frequencies. However, differences in the obtained conductivities depending on the perturbation amplitude are negligible regardless of the measuring temperature, when considering the average of at least three samples (Figure 6b). On the other hand, the activation barriers seem to be more sensitive to the amplitude applied as an effective lowering of the activation barrier is observed at 50 mV (Figure 6c). However, if we consider the average of at least three pellets there is no statistical difference between the amplitudes considered in this study.

3.5. Effect of Pressure During Measurement

Together with the pouched cell setup, Li_6PS_5Br pellets were investigated in the TSC-battery cell under the same measurement conditions. For the third measurement setup we used a

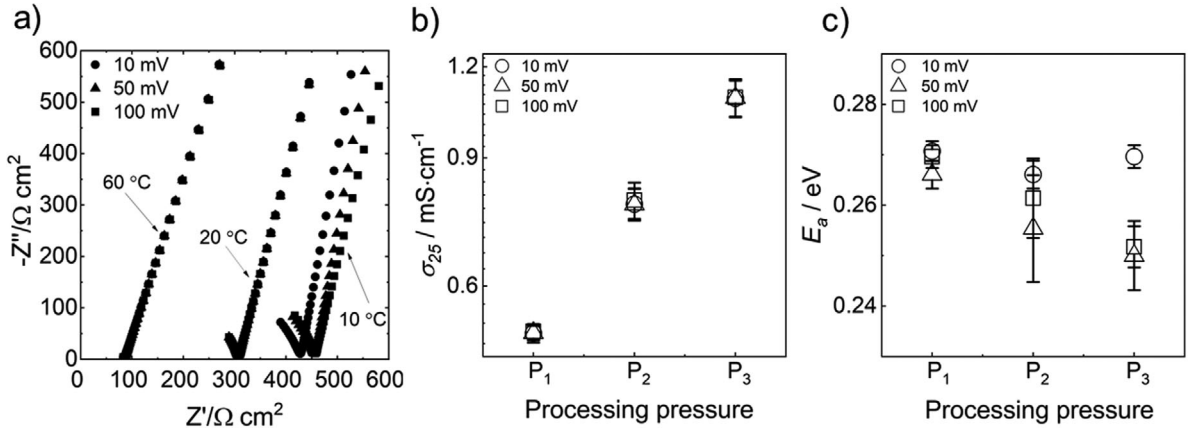

Figure 6. a) Representative spectra in a Nyquist plot of a Li_6PS_5Br sample pelletized at 320 MPa (P_3) measured at 10, 20, and 60 °C and 10, 50, and 100 mV perturbation amplitudes in a pouched cell. Comparison of average b) total ionic conductivities at 25 °C and c) activation barriers of Li_6PS_5Br pressed at 3 different isostatic pressures measured at 10, 50, and 100 mV perturbation amplitudes during the 1st heating cycle. Dashed lines are depicted to help to separate different processing pressures. The error bars represent the standard deviation of three pellets per processing pressure.

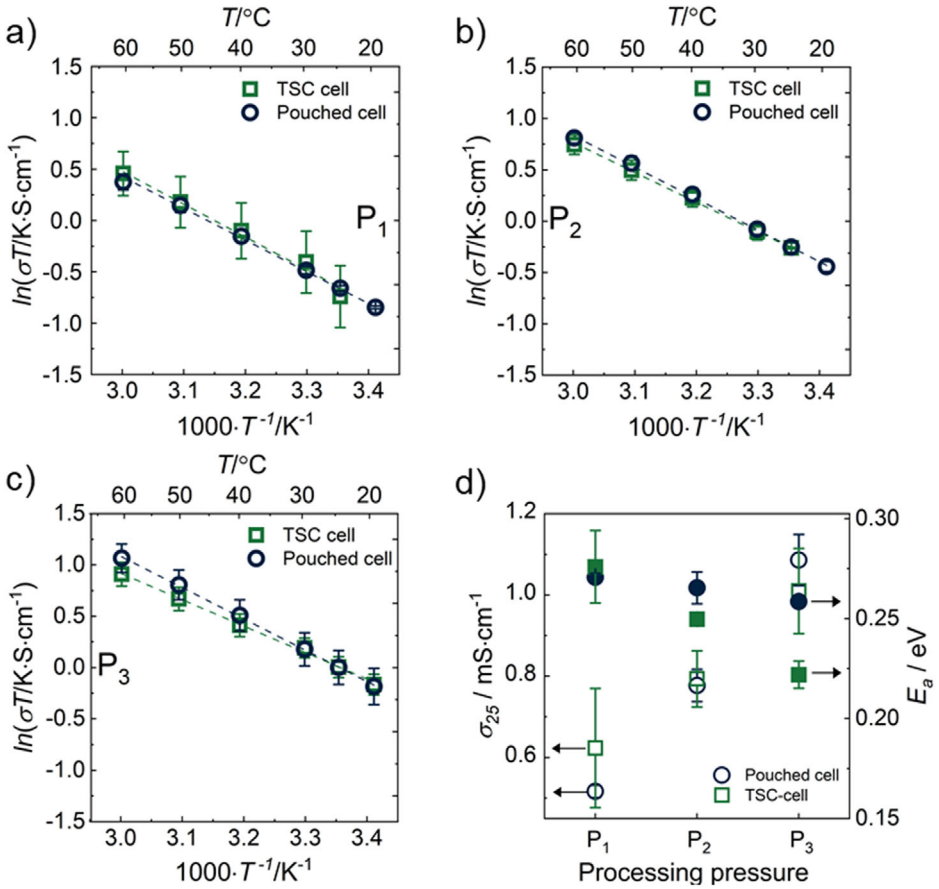

Figure 7. Arrhenius plots of total ionic conductivities of two measurement setups, both measured at 10 mV perturbation amplitude for processing pressures a) 160 MPa (P_1), b) 235 MPa (P_2) and c) 320 MPa (P_3). Dashed lines are the linear fits to the data. d) Comparison of the activation barriers obtained between the two setups as a function of processing pressure. The error bars represent the standard deviation of three pellets per processing pressures.

CompreDrive, where Li_6PS_5Br powders were in-situ pelletized and measured subsequently. The aim of comparing three setups is to determine how much the measurement setup influences the resulting ionic conductivities. In comparison to the pouched cell setup (with minimal applied pressure), TSC-cell compress the electrolyte between rigid electrodes (with 1.13 MPa of applied pressure), enhancing electrode contact to the sample. **Figure 7** represents comparison of the Arrhenius plots of total ionic conductivities obtained from pouched cell and TSC battery cell measured at 10 mV perturbation amplitude using gold sputtered contacts.

As can be seen, no significant difference in the average total ionic conductivities are quantified. However, the E_a of samples measured in TSC-cell are notably decreasing (E_a at P_1 is statistically greater than at P_3), whereas in the pouched cell setup we do not observe such a trend (Figure 7d). Additional pressure during the measurement improves electrode-electrolyte contact, particularly for electrodes in foil or sheet form. When coating pellets with a good contact material such as gold (Au), a relatively low contact pressure is already sufficient to obtain reliable results. In this study, we found no significant effect of additional pressure applied during the measurement on the total conductivity of pre-pelletized electrolytes.

Compared to the first and second setup, the third setup operates at significantly higher pressures and does not require additional electrodes as the hard metal pistons (tungsten carbide (90%) + cobalt (10%)) of the cell serve as electrodes. The application of higher pressure reduces contact resistance, simplifying sample preparation since pelletizing occurs in-situ. When starting from the powder form, the sample is gradually pelletized, resulting in increased density, reduced porosity, and enhanced ionic conductivity. Impedance data were collected at different pressure stages after equilibration to monitor resistance changes of the sample during densification and determine the minimum pressure required for adequate densification. The highest applied pressure, 400 MPa, was defined as the sample processing pressure. After reaching this maximum, measurements were repeated with the now compacted pellet to assess the effect of applied pressure on contact resistance. The effect of pressure during the measurement is shown in **Figure 8a**.

When reducing the pressure, it becomes clear that a minimum pressure of 200 MPa is required to maintain good contact, as lower pressures led to a sharp increase in resistance. Finally, at this optimal contact pressure, impedance data were recorded at different temperatures to determine the activation energy.

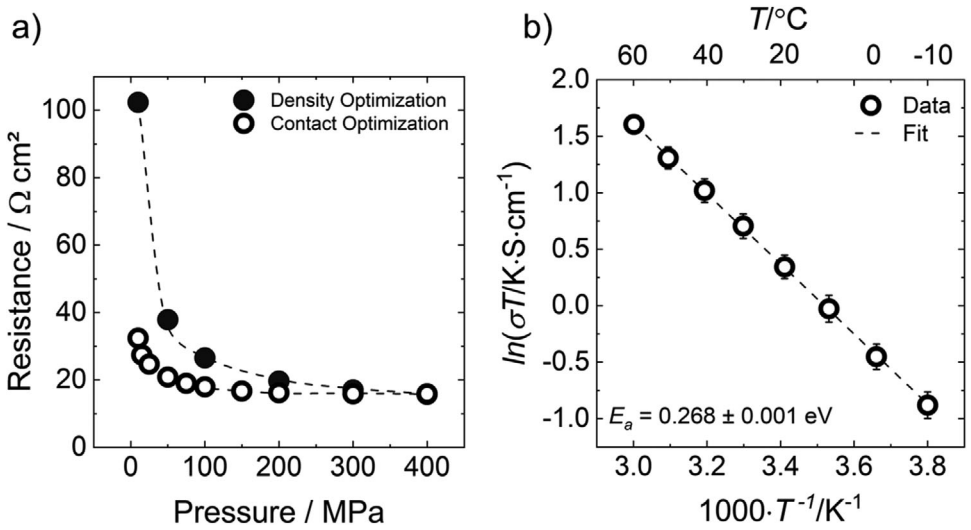

Figure 8. a) Influence of the pressure on resistance obtained from the CompreDrive on a single representative pellet; b) Arrhenius plot of average total ionic conductivity of Li_6PS_5Br obtained from the CompreDrive. The error bars represent the standard deviation of three samples compacted at 400 MPa and measured at 200 MPa.

Note that the final pellet dimensions can only be determined after retrieval from the cell, making it impractical to calculate conductivities during the compaction process. For samples compacted at 400 MPa and measured at 200 MPa, a conductivity of 1.6 ± 0.2 mS·cm^{-1} and an activation energy of 0.268 ± 0.001 eV were obtained. The relative density achieved at the maximum processing pressure of 400 MPa was 90 ± 4%. Taken together, pressure during the measurement applied by TSC cell on already isostatically pelletized sample did not affect resulting conductivities. Uniaxial in-situ pelletizing at 400 MPa with additional 200 MPa measurement conducted by CompreDrive pressure increased the conductivity by ≈47%.

While our study focused mostly on Li_6PS_5Br, the observed effects of processing pressure thresholds and measurement conditions are broadly relevant and applicable to other sulfide-based solid electrolytes. For example, Doux et al.[44] reported that with applying higher processing pressure of 370 MPa the conductivity of Li_6PS_5Cl significantly increased improving the cycling performance. Authors also underlined that the measurement/stack pressure had no major influence on the performance of the Li_6PS_5Cl containing cells.[44] In controversy, an interlaboratory study showed the possible increase with external pressure applied during the measurement mostly in a press cell configuration.[11] Faka et al.[45] reported that due to increased activation volume in Li_6PS_5Br, pressure during measurement suppresses Li^+ conductivity and stated that processing and measurement pressures must be designed carefully to maintain the superionic performance of the material.[45] All of the findings discussed in this paper, including our work, show that, while specific thresholds may vary by composition or microstructure, the underlying trends are consistent across the sulfide family. Moreover, standardizing the processing and measurement conditions for electrochemical impedance spectroscopy of sulfide-based solid electrolytes would provide a critical foundation for improving the overall performance and comparability of ASSBs. As demonstrated in the work of Bielefeld et al.,[46] numerical simulations show how variations in ion transport properties and microstructure significantly impact the performance of cathode composites and the cell in general. In general, if thick electrodes (in the order of 100 µm) and C-rates above 1C are desired, solid electrolytes must have ionic conductivities greater than 10 mS·cm^{-1}. Since the impedance spectra of solid electrolytes becomes less resolved as their total resistivity decreases, i.e., the high-frequency arc is poorly defined, a standardized and robust protocol for the determination and benchmarking of novel solid electrolytes materials is necessary. Our study provides the foundation for such a protocol with clear guidelines on how to process the samples, how to contact the samples, how to conduct the impedance measurement itself as well as clear suggestions on how to analyze the data. With a robust protocol established for solid electrolyte characterization, subsequent standardization of ASSB assembly and cycling procedures can further accelerate reliable development in the field.

4. Conclusion

This study aimed to establish a comprehensive methodology for the evaluation of ionic conductivities of solid electrolytes using thiophosphate lithium argyrodite (Li_6PS_5Br) as an example. The influence of isostatic and uniaxial processing pressures, measurement and analyses conditions of electrochemical impedance spectroscopy (EIS), using three measurement setups on the nominally equal samples were evaluated systematically. Our findings help us propose the following protocol/guidelines in characterizing lithium argyrodite solid electrolytes:

1) For processing lithium argyrodite solid electrolytes, we recommend using isostatic pressing at 320 MPa or higher. If the isostatic pressing is not available, the uniaxial compression at higher pressures (above 320 MPa) is recommended.
2) Careful attention must be paid not just to the electrode material but also to the contacting technique. Sputtered metal

electrodes such as Au or Pt should be preferred, wherever possible, to ensure the accuracy, reproducibility, and comparability of ionic conductivity measurements.

3) We suggest using the smaller perturbation amplitude (10 mV) to ensure that the system remains within the linear regime. To ensure reliable data, the available linearity test alongside EIS should be performed – some potentiostats support total harmonic distortion analysis. However, if high amplitudes are necessary, the analysis should account for the possibility of nonlinear contributions and advanced techniques like Fourier transform EIS should be applied to separate linear and nonlinear components.
4) If the pressure used for isostatic pressing of Li_6PS_5Br samples is lower than 160 MPa or the pellets were pressed uniaxially, the use of additional pressure during the measurement must be considered. Moreover, additional pressure during the measurement might be helpful for the electrode-electrolyte contact in case of electrode in a foil or sheet forms. For samples pressed at high pressures (320 MPa and above) and the electrode is sputtered evenly, the additional pressure during the measurement does not have an effect on resulting conductivities.
5) A uniaxial setup with a pressure control can be beneficial, as it allows precise determination of the optimal processing pressure and the saturation point for contact resistance reduction—minimizing additional impedance effectively. These parameters are often specific to each electrolyte sample and can vary between batches due to factors such as particle size distribution or purity.
6) The exact procedure of sample processing, measurement conditions and the fitting methods should be reported. Moreover, we strongly recommend triplicating results to ensure reproducibility.

The influence of the studied parameters in some cases might be within the error, but combination of all the factors could be the reason of the lack of reproducibility and standardized procedure. We hope that our findings offer new tools to enable the standardization of ionic transport in solid electrolytes.

Supporting Information

Supporting Information is available from the Wiley Online Library or from the author.

Acknowledgements

The authors the Bundesministerium für Bildung und Forschung (BMBF) for financial support to conduct this study, project 03XP0497B for authors F.K. and N.M.V.-B. and project 03XP0497A for authors L.P. and M.D.

Conflict of Interest

M.D. and L.P. work for the company rhd instruments GmbH & Co. KG which is selling the test cells TSC battery and CompreCell 12C as well as the testing station CompreDrive that were used for some of the measurements presented in this work. Furthermore, the same company is selling the software RelaxIS 3 that was used for EIS data analysis.

Author Contributions

F.K. performed investigation, validation, data curation, formal analysis, visualization, writing – original draft preparation, writing – review & Editing. L.P. performed investigation, validation, data curation, formal analysis, visualization, writing – review & editing. M.D. performed conceptualization, funding acquisition, methodology, project administration, resources, supervision, writing – review & editing. N.M.V.-B. performed conceptualization, funding acquisition, methodology, project administration, resources, supervision, visualization, writing – review & editing.

Data Availability Statement

The data that support the findings of this study are openly available in Jülich Data at https://doi.org/10.26165/JUELICH-DATA/FMIHIQ.

Keywords

electrochemical impedance spectroscopy, ionic conductivity, SE, solid electrolyte

Received: April 15, 2025
Revised: June 27, 2025
Published online: August 8, 2025

[1] U. Ulissi, R. Raccichini, *Front. Nanosci.* **2021**, *19*, 1.
[2] J. Janek, W. G. Zeier, *Nat. Energy* **2023**, *8*, 230.
[3] J. Janek, W. G. Zeier, *Nat. Energy* **2016**, *1*, 1.
[4] Z. Zhang, Y. Shao, B. Lotsch, Y.-S. Hu, H. Li, J. Janek, L. F. Nazar, C.-W. Nan, J. Maier, M. Armand, L. Chen, *Energy Environ. Sci.* **2018**, *11*, 1945.
[5] S. Puls, E. Nazmutdinova, F. Kalyk, H. M. Woolley, J. F. Thomsen, Z. Cheng, A. Fauchier-Magnan, A. Gautam, M. Gockeln, S.-Y. Ham, M. T. Hasan, M.-G. Jeong, D. Hiraoka, J. S. Kim, T. Kutsch, B. Lelotte, P. Minnmann, V. Miß, K. Motohashi, D. L. Nelson, F. Ooms, F. Piccolo, C. Plank, M. Rosner, S. E. Sandoval, E. Schlautmann, R. Schuster, D. Spencer-Jolly, Y. Sun, B. S. Vishnugopi, et al., *Nat. Energy* **2024**, *9*, 1310.
[6] R. Tatara, P. Karayaylali, Y. Yu, Y. Zhang, L. Giordano, F. Maglia, R. Jung, J. P. Schmidt, I. Lund, Y. Shao-Horn, *J. Electrochem. Soc.* **2019**, *166*, A5090.
[7] L. Zhu, Y. Wang, J. Chen, W. Li, T. Wang, J. Wu, S. Han, Y. Xia, Y. Wu, M. Wu, F. Wang, Y. Zheng, L. Peng, J. Liu, L. Chen, W. Tang, *Sci. Adv.* **2022**, *8*, 1.
[8] L. Hu, J. Wang, K. Wang, Z. Gu, Z. Xi, H. Li, F. Chen, Y. Wang, Z. Li, C. Ma, *Nat. Commun.* **2023**, *14*, 1.
[9] A. Manthiram, X. Yu, S. Wang, *Nat. Rev. Mater.* **2017**, *2*, 1.
[10] K. J. Kim, M. Balaish, M. Wadaguchi, L. Kong, J. L. M. Rupp, *Adv. Energy Mater.* **2021**, *11*, 1.
[11] S. Ohno, T. Bernges, J. Buchheim, M. Duchardt, A-.K. Hatz, M. A. Kraft, H. Kwak, A. L. Santoscha, Z. Liu, N. Minafra, F. Tsuji, A. Sakuda, R. Schlem, S. Xiong, Z. Zhang, P. Adelhelm, H. Chen, A. Hayashi, Y. S. Jung, B. V. Lotsch, B. Roling, N. M. Vargas-Barbosa, W. G. Zeier, *ACS Energy Lett.* **2020**, *5*, 910.
[12] P. Perrenot, A. Fauchier-Magnan, M. Mirolo, L. Lecarme, P.-H. Jouneau, A. Boulineau, P. Bayle-Guillemaud, C. Villevieille, *Adv. Funct. Mater.* **2024**, *34*, 1.
[13] M. Cronau, M. Szabo, C. König, T. B. Wassermann, B. Roling, *ACS Energy Lett.* **2021**, *6*, 3072.
[14] I. V. Krasnikova, M. A. Pogosova, A. O. Sanin, K. J. Stevenson, *Chem. Mater.* **2020**, *32*, 2232.

[15] M. Müller, H. Auer, A. Bauer, S. Uhlenbruck, M. Finsterbusch, K. Wätzig, K. Nikolowski, S. Dierickx, D. Fattakhov-aRohlfing, O. Guillon, A. Weber, *J. Power Sources* **2022**, *531*, 1.
[16] J. Min Goh, C. Eluagu, J. Babauta, M. E. Orazem, *J. Electrochem. Soc.* **2024**, *171*, 036508.
[17] J. J. Giner-Sanz, E. M. Ortega, V. Pérez-Herranz, *Electrochim. Acta* **2015**, *186*, 598.
[18] A. C. Lazanas, M. I. Prodromidis, *ACS Measurement Sci. Au* **2023**, *3*, 162.
[19] S. Wang, J. Zhang, O. Gharbi, V. Vivier, M. Gao, M. E. Orazem, *Nat. Rev. Methods Primers* **2021**, *1*, 1.
[20] L. Zhang, Y. Dai, C. Li, Y. Dang, R. Zheng, Z. Wang, Y. Wang, Y. Cui, H. Arandiyan, Z. Shao, H. Sun, Q. Zhuang, Y. Liu, *Energy Storage Mater.* **2024**, *69*, 1.
[21] B. Y. Chang, S. M. Park, *Annu. Rev. Anal. Chem.* **2010**, *3*, 207.
[22] P. Vadhva, J. Hu, M. J. JOhnson, R. Stocker, M. Braglia, D. J. L. Brett, A. J. E. Rettie, *ChemElectroChem* **2021**, *8*, 1930.
[23] Y. Wang, R. Lim, K. Larson, A. Knab, D. Fontecha, S. Caverly, J. Song, C. Park, P. Albertus, G. W. Rubloff, S. B. Lee, A. C. Kozen, *ChemSusChem* **2024**, *17*, 202400718.
[24] V. Faka, M. T. Agne, M. A. Lange, D. Daisenberger, B. Wankmiller, S. Schwarzmüller, H. Huppertz, O. Maus, B. Helm, T. Böger, J. Hartel, J. M. Gerdes, J. J. Molaison, G. Kieslich, M. R. Hansen, W. G. Zeier, *J. Am. Chem. Soc.* **2024**, *146*, 1710.
[25] Q. A. Tran, M. Agrawal, M. Häusler, J. Hörmann, M. S. Moqadam, G. J. Redhammer, I. S. Ellingsen, M. M. Ud Din, P. E. Vullum, R. Zettl, T. Danner, A. Latz, V. Hennige, R. Brunner, D. Rettenwander, *Adv. Mater.* **2025**, *130*, 1.
[26] A. Sakuda, A. Hayashi, M. Tatsumisago, *Sci. Rep.* **2013**, *3*, 1.
[27] C. Sedlmeier, T. Kutsch, R. Schuster, L. Hartmann, R. Bublitz, M. Tominac, M. Bohn, H. A. Gasteiger, *J. Electrochem. Soc.* **2022**, *169*, 070508.
[28] T. Ates, A. Neumann, T. Danner, A. Latz, M. Zarrabeitia, D. Stepien, A. Varzi, S. Passerini, *Adv. Sci.* **2022**, *9*, 1.
[29] T. Kim, S. Hyeok Ahn, Y-.Y. Song, B. J. Park, C. Lee, A. Choi, M-.H. Kim, D-.H. Seo, S-.K. Jung, H-.W. Lee, *Angew. Chem,: Int. Ed.* **2023**, *62*, 1.
[30] Y. Huang, R. Černý, C. Battaglia, A. Remhof, *J. Mater. Sci.* **2023**, *58*, 7398.
[31] Z. Wei, Y. Ren, M. Wang, J. He, W. Huo, H. Tang, *Nanoscale Res. Lett.* **2020**, *15*, 1.
[32] A. Mormeneo-Segarra, S. Ferrer-Nicomedes, N. Vicente-Agut, A. Barba-Juan, *Mater. Adv.* **2024**, *5*, 6554.
[33] P. Adeli, J. D. Bazak, K. H. Park, I. Kochetkov, A. Huq, G. R. Goward, L. F. Nazar, *Angew. Chem.* **2019**, *131*, 8773.
[34] I. Hanghofer, M. Brinek, S. L. Eisbacher, B. Bitschnau, M. Volck, V. Hennige, I. Hanzu, D. Rettenwander, H. M. R. Wilkening, *Phys. Chem. Chem. Phys.* **2019**, *21*, 8489.
[35] H. J. Deiseroth, et al., *Angew. Chem,: Int. Ed.* **2008**, *47*, 755.
[36] M. A. Kraft, S. P. Culver, M. Calderon, F. Böcher, T. Krauskopf, A. Senyshyn, C. Dietrich, A. Zevalkink, J. Janek, W. G. Zeier, *J. Am. Chem. Soc.* **2017**, *139*, 10909.
[37] J. Wallauer, RelaxIS Impedance Spectrum Analyses, User's Manual **2013**, Preprint at http://www.rhd-instruments.com.
[38] Z. Xiao, H. Wang, N. Cai, Y. Li, K. Xiang, W. Wei, T. Ye, Z. Zhang, S. Wang, Z. Tang, *Nano Res.* **2024**, *17*, 6139.
[39] T. Famprikis, P. Canepa, J. A. Dawson, M. S. Islam, C. Masquelier, *Nat. Mater.* **2019**, *18*, 1278.
[40] C. Yu, J. Hageman, S. Ganapathy, L. van Eijck, L. Zhang, K. R. Adair, X. Sun, M. Wagemaker, *J. Mater. Chem. A* **2019**, *7*, 10412.
[41] L. Zhou, K.-H. Park, X. Sun, F. Lalère, T. Adermann, P. Hartmann, L. F. Nazar, *ACS Energy Lett.* **2019**, *4*, 265.
[42] A. Gautam, M. Sadowski, M. Ghidiu, N. Minafra, A. Senyshyn, K. Albe, W. G. Zeier, *Adv. Energy Mater.* **2021**, *11*, 1.
[43] J. J. Giner-Sanz, E. M. Ortega, V. Pérez-Herranz, *Electrochim. Acta* **2016**, *211*, 1076.
[44] J.-M. Doux, Y. Yang, D. H. S. Tan, H. Nguyen, E. A. Wu, X. Wang, A. Banerjee, Y. S. Meng, *J. Mater. Chem. A* **2020**, *8*, 5049.
[45] V. Faka, M. T. Agne, P. Till, T. Bernges, M. Sadowski, A. Gautam, K. Albe, W. G. Zeier, *Energy Adv.* **2023**, *2*, 1915.
[46] A. Bielefeld, D. A. Weber, J. Janek, *ACS Appl. Mater. Interfaces* **2020**, *12*, 12821.